Available at https://journalenrichment.com/index.php/jr/

Enrichment: Journal of Multidisciplinary Research and Development

Analysis Of Convective Cloud Distribution Patterns Using The Himawari-9 Satellite Red Green Blue (Rgb) Method In The Cenderawasih Bay Coastal Region In 2023

Eusebio Andronikos Sampe[1], Noorlaila Hayati[2]
[1]Badan Meteorologi, Klimatologi, dan Geofisika Indonesia, Nabire, Indonesia
[2]Institut Teknologi Sepuluh Nopember, Sukulilo Surabaya, Indonesia
E-mail: eusebio.sampe@bmkg.go.id

ABSTRACT

Cenderawasih Bay, located near the equator, is characterized by a local rainfall pattern largely influenced by the development of convective clouds along its coastal areas. This study aims to analyze the distribution patterns of convective clouds in the coastal region of Cenderawasih Bay using data from the Himawari-9 meteorological satellite. The research method employed the RGB (Red Green Blue) composite technique using SATAID software to visualize and interpret convective cloud dynamics. The results show that during the June 2023 period, cloud-top temperatures ranged from -50°C to -70°C, with cloud movements predominantly from east to west. Convective clouds were primarily observed over the coastal areas of Manokwari, Biak, Serui, and Nabire, with cloud growth occurring mostly at night until early morning. The vertical development of clouds in this period reached heights between 3.1 km and 15.5 km. In contrast, during November 2023, convective cloud activity was significantly lower, mainly limited to Manokwari and Biak, with similar nocturnal growth patterns and cloud heights ranging from 1.8 km to 15.1 km. The RGB day convective storms composite effectively identified ice particles in cloud tops, linking cloud distribution with potential rainfall events. The RGB 24-hour microphysics product was also useful in monitoring cloud-top temperature variations to assess severe weather potential. These findings demonstrate the effectiveness of satellite-based RGB analysis in monitoring convective activity and its relation to localized precipitation, providing valuable insight for weather forecasting and disaster preparedness in the region.

Keywords: *convective clouds, RGB method, SATAID, Cenderawasih Bay*

INTRODUCTION

Convective clouds are clouds that cause localized rainfall of moderate to heavy intensity as a result of unstable convection processes in the atmosphere. Convective clouds play an important role in atmospheric dynamics and the hydrological cycle capable of producing heavy rainfall (Christensen & Driver, 2021; Nie et al., 2023; Xiao et al., 2024). Common and dominant types of convective clouds that develop in the tropics are cumulus and cumlunimbus clouds, which can appear separately or in clusters (Ninggar et al., 2023). The use of meteorological satellites in analyzing convective clouds has been carried out by the Meteorology, Climatology and Geophysics Agency (BMKG) in the field of meteorology in observing the distribution of convective clouds in the growth phase, mature to decay in real time using the Himawari satellite (Ramdani, 2021; Romero Jure et al., 2023).

The coastal areas of Cenderawasih bay used as the location of this study are Nabire, Biak, Yapen (Serui) and Manokwari. In the central plains of Cenderawasih bay, the JJA rain pattern (June, July, August) becomes strongest in the northern lowlands of the Nabire cluster and the Biak, Yapen cluster in the Cenderawasih bay islands. Especially for the Manokwari area, it forms a monsoon rain pattern that slopes from MAM (March, April, May) to SON (September, October, November) (Nugroho, 2017; Rouw et al., 2014; Yoshida & Asano, 2015). Thus it can be interpreted that the coastal area of Cenderawasih Bay is dominant in the middle of the year in June, July and August there is a significant increase in rainfall while in September, October and November there is a decrease in rainfall. Specifically for the Cenderawasih Bay area in the Papua region, it has a characteristic weather condition with high growth of convective clouds which causes bad weather phenomena, one of which is heavy rain or extreme rain and the absence of a clear pattern of convective cloud distribution because almost all year round rainfall is quite high, so researchers are interested in studying this, namely examining the distribution pattern of convective clouds on the Himawari-9 satellite in the coastal region of Cenderawasih Bay (Kikuchi & Wang, 2015; Sugiura & Nakajima, 2015).

Previous studies have examined the role of convective cloud growth using satellite imagery to improve rainfall prediction accuracy. For instance, Setiawan et al. (2020) analyzed the distribution and movement of convective clouds in Indonesia using Himawari-8 satellite imagery, showing the relevance of RGB composite techniques in visualizing cloud dynamics for weather forecasting. Similarly, Sari et al. (2021) investigated the vertical structure of convective clouds in West Papua and confirmed a correlation between cloud-top temperature and precipitation intensity. However, existing research has not yet provided a focused temporal and spatial analysis on convective cloud behavior specifically in the coastal regions of Cenderawasih Bay using Himawari-9 satellite data. The novelty of this study lies in its comprehensive time-series analysis of cloud growth phases and cloud-top temperature contours across distinct coastal sub-regions Manokwari, Biak, Yapen, and Nabire during contrasting periods (June and November), which is crucial for identifying rainfall anomalies and enhancing localized weather forecasting (Ishii & Kachi, 2015; Matsui & Masunaga, 2015; Taniguchi & Nakazawa, 2016).

The purpose of this research is knowing the distribution pattern of convective cloud distribution, analyzing the time series of convective cloud development, knowing the position of the region, analyzing the temperature contour of the peak of convective clouds, knowing the direction of movement, analyzing the growth phase, mature phase and decay phase and analyzing whether there is a relationship between the convective cloud distribution variable and the rainfall variable (Kawamoto & Nakajima, 2016; Yamada & Sato, 2017). The benefit of this research lies in its contribution to understanding local weather dynamics in Papua, particularly for early warning systems, disaster preparedness, and enhancing the accuracy of short-term rainfall forecasts. These insights are valuable for meteorological agencies, local governments, and communities in minimizing risks related to extreme weather events (Fujita & Yasunari, 2017; Ohashi & Kida, 2018).

METHOD

The research method used in this research is the Red Green Blue (RGB) method of satellite image modification or interpretation techniques that are originally black and white into color by utilizing 3 (three) primary colors, namely red (red), green (green) and blue (blue) (Huda & Mulya, 2022). In satellite image data processing, RGB techniques are used to combine several channels of different wavelengths in order to obtain an image product that contains better information than that obtained from a single channel image (Paski et al., 2019). SATAID is used to display binary data from the Himawari satellite into images. Using SATAID, RGB images are easily organized and analyzed (Saragih & al., 2021).

RESULTS AND DISCUSSION

Times Series and convective cloud regions

June 2023 period

Based on the results of running the RGB day convective storms scheme, RGB 24-hour Microphysics and RGB Air Mass, it is known that in the morning to early morning period (09.00 - 03.00 WIT) there is a dominant deep precipitating cloud with large ice Cb Cloud, there are thick clouds with high peaks (Cumulunimbus), there are white to dark green cloud patterns, on the coastal areas of the western, central, southern and eastern bays of West Papua Manokwari, Biak, Serui and Nabire.

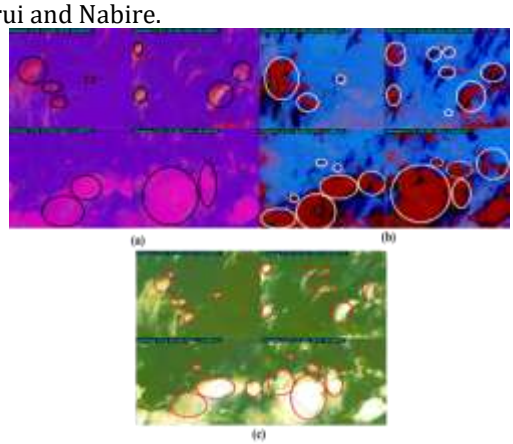

Figure 1. (a) RGB of Convective Storm for a Day, (b) RGB of Microphysics for 24 hours, (c) RGB of Air Mass for June 10, 2023

Based on the results of running the RGB day convective storms scheme, RGB 24-hour Microphysics and RGB Air Mass, it is known that in the morning to early morning period (09.00 - 03.00 WIT), dominant is deep precipitating cloud with large ice Cb Cloud, there are thick clouds with high peaks (Cumulunimbus), there are

white to dark green cloud patterns, on the western, central, southern and eastern coastal areas of West Papua Cenderawasih Bay Manokwari, Biak, Serui and Nabire.

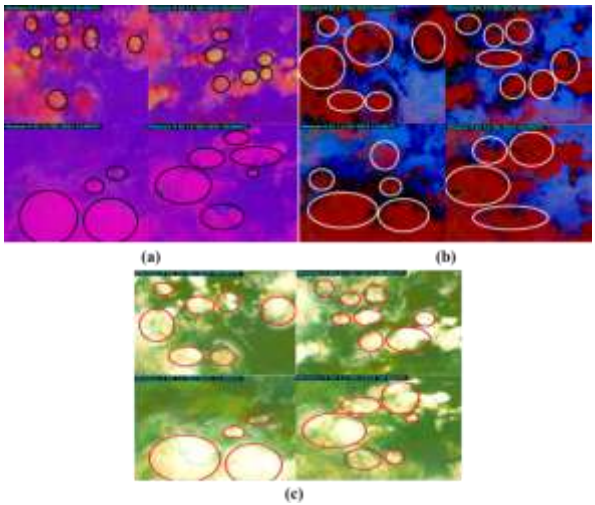

Figure 2. (a) RGB Day Convective Storms, (b) RGB 24-hour Microphysics, (c) RGB Air Mass for June 11, 2023

Based on the results of running the RGB day convective storms scheme, RGB 24-hour Microphysics and RGB Air Mass, it is known that in the morning to early morning period (09.00 - 03.00 WIT), dominant is deep precipitating cloud with large ice Cb Cloud, there are thick clouds with high peaks (Cumulunimbus), there are white to dark green cloud patterns, on the western, central, southern and eastern coastal areas of West Papua Cenderawasih Bay Manokwari, Biak, Serui and Nabire.

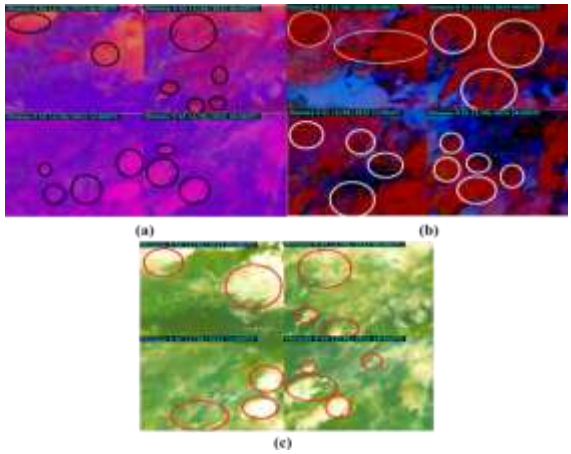

Figure 3. (a) RGB Day Convective Storms, (b) RGB 24-hour Microphysics, (c) RGB Air Mass for June 12, 2023

November 2023 period

Based on the results of running the RGB day convective storms scheme, RGB 24-hour Microphysics and RGB Air Mass, it is known that in the morning to early morning period (09.00 - 03.00 WIT), there are several deep precipitating clouds with large ice Cb Cloud and several small and large ice particles, dominant there are several thick clouds with high peaks (Cumulunimbus), dominant there are white to dark green cloud patterns, which indicate the content of warm air masses characterized by high water vapor content. on the west and central coastal areas of Cenderawasih Bay in the Manokwari, Biak and Serui regions.

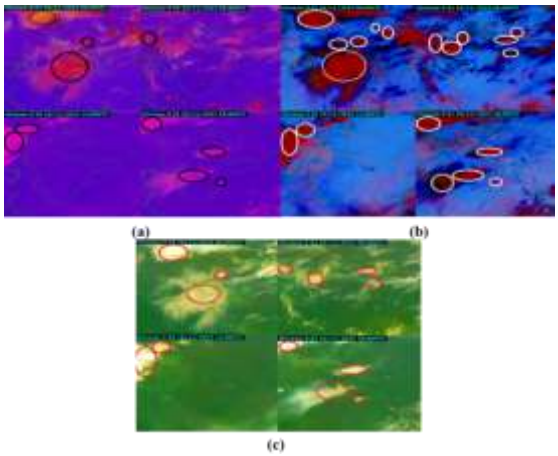

Figure 4. RGB Day Convective Storms, (b) RGB 24-hour Microphysics, (c) RGB Air Mass for November 10, 2023

Based on the results of running the RGB day convective storms scheme, RGB 24-hour Microphysics and RGB Air Mass, it is known that in the morning to early morning period (09.00 - 03.00 WIT), there are several deep precipitating clouds with large ice Cb Cloud and several small and large ice particles, dominant there are several thick clouds with high peaks (Cumulunimbus), dominant there are white to dark green cloud patterns, which indicate the content of warm air masses characterized by high water vapor content. on the west and central coastal areas of Cenderawasih Bay in the Manokwari, and Nabire regions.

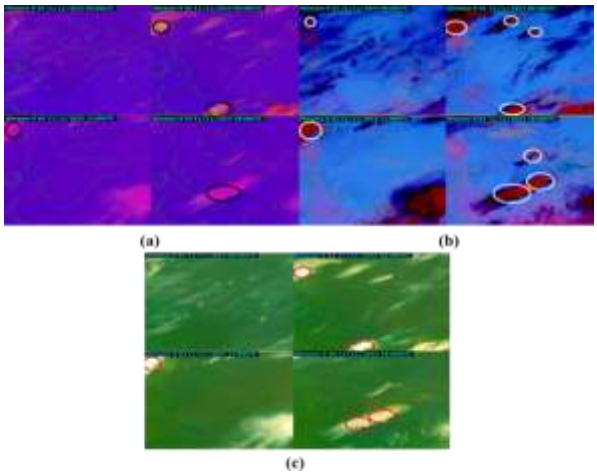

Figure 5. RGB Day Convective Storms, (b) RGB 24-hour Microphysics, (c) RGB Air Mass for November 11, 2023

Based on the results of running the RGB day convective storms scheme, RGB 24-hour Microphysics and RGB Air Mass, it is known that in the morning to early morning period (09.00 - 03.00 WIT), there are several deep precipitating clouds with large ice Cb Cloud and several small and large ice particles, dominant there are several thick clouds with high peaks (Cumulunimbus), dominant there are white to dark green cloud patterns, which indicate the content of warm air masses characterized by high water vapor content. on the west and central coastal areas of Cenderawasih Bay in the Manokwari, and Nabire regions.

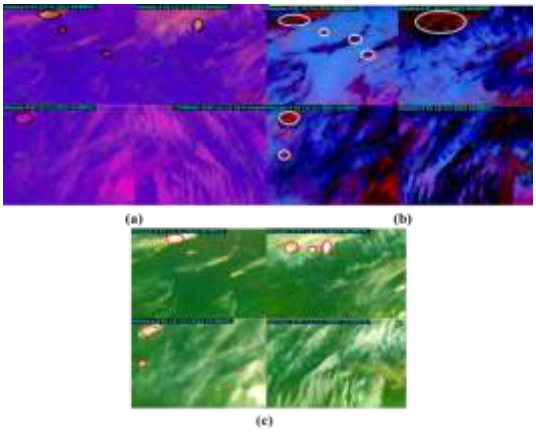

Figure 6. RGB Day Convective Storms, (b) RGB 24-hour Microphysics, (c) RGB Air Mass for November 12, 2023

The position of the region where convective cloud growth is dominant
June 2023 period

From the data in Figure 7, the position of the convective cloud area in the period of June 10-12, 2023 from 3 (three) red green blue (RGB) schemes used, it was found that in the morning to early morning time period (09.00 - 03.00 WIT) there were dominant convective clouds in the coastal areas of West Papua Manokwari, Biak, Serui and Nabire to Waropen.

Skema RGB	Waktu Penelitian Tanggal 10 Juni 2023	
	Waktu (WIT)	Posisi Wilayah
1. RGB *Day Convective Storms* *Deep precitipating cloud with small & large ice Cb Cloud*	09.00 - 03.00	Papua Barat, Manokwari, Serui & Nabire hingga Waropen
2. RGB 24-*hour Microphysics* Awan tebal dengan puncak yang tinggi (Cumulunimbus)	09.00 - 03.00	Papua Barat Manokwari, Biak, Serui & Nabire hingga Waropen
3. RGB *Air Mass* Kandungan massa udara hangat Kandungan uap air yang tinggi	09.00 - 03.00	Papua Barat Manokwari, Biak, Serui & Nabire hingga Waropen

Skema RGB	Waktu Penelitian Tanggal 11 Juni 2023	
	Waktu (WIT)	Posisi Wilayah
1. RGB *Day Convective Storms* *Deep precitipating cloud with small & large ice Cb Cloud*	09.00 - 03.00	Papua Barat Manokwari, Biak, Serui & Nabire hingga Waropen
2. RGB 24-*hour Microphysics* Awan tebal dengan puncak yang tinggi (Cumulunimbus)	09.00 - 03.00	Papua Barat Manokwari, Biak, Serui & Nabire hingga Waropen
3. RGB *Air Mass* Kandungan massa udara hangat Kandungan uap air yang tinggi	09.00 - 03.00	Papua Barat Manokwari, Biak, Serui & Nabire hingga Waropen

Skema RGB	Waktu Penelitian Tanggal 12 Juni 2023	
	Waktu (WIT)	Posisi Wilayah
1. RGB *Day Convective Storms* *Deep precitipating cloud with small & large ice Cb Cloud*	09.00 - 03.00	Papua Barat Manokwari, Serui & Nabire hingga Waropen
2. RGB 24-*hour Microphysics* Awan tebal dengan puncak yang tinggi (Cumulunimbus)	09.00 - 03.00	Papua Barat Manokwari, Biak, Serui & Nabire hingga Waropen
3. RGB *Air Mass* Kandungan massa udara hangat Kandungan uap air yang tinggi	09.00 - 03.00	Papua Barat Manokwari, Biak, Serui & Nabire hingga Waropen

Figure 7. Summary of the position of the convective cloud area for the period June 10 - 12, 2023

November 2023 period

From the data in Figure 8, the time series of convective clouds in the period of November 10-12, 2023 from the 3 (three) red green blue (RGB) schemes used, it was found that in the morning to early morning time period (09.00 - 03.00 WIT) there were only a few convective clouds (insignificant) dominant in the coastal areas of the western, central and northern Cenderawasih bay of West Papua Manokwari and Biak.

Skema RGB	Waktu Penelitian Tgl 10 Nopember 2023	
	Waktu (WIT)	Posisi Wilayah
1. RGB *Day Convective Storms* *Deep precitipating cloud with small & large ice Cb Cloud*	09.00 - 03.00	Manokwari & Serui
2. RGB 24-*hour Microphysics* Awan tebal dengan puncak yang tinggi (Cumulunimbus)	09.00 - 03.00	Papua Barat Manokwari, Biak & Serui
3. RGB *Air Mass* Kandungan massa udara hangat Kandungan uap air yang tinggi	09.00 - 03.00	Papua Barat Manokwari, Biak & Serui

Skema RGB	Waktu Penelitian Tgl 11 Nopember 2023	
	Waktu (WIT)	Posisi Wilayah
1. RGB *Day Convective Storms* *Deep precitipating cloud with small & large ice Cb Cloud*	09.00 - 03.00	Manokwari & Nabire
2. RGB 24-*hour Microphysics* Awan tebal dengan puncak yang tinggi (Cumulunimbus)	09.00 - 03.00	Papua Barat Manokwari, Biak, Serui & Nabire
3. RGB *Air Mass* Kandungan massa udara hangat Kandungan uap air yang tinggi	09.00 - 03.00	Papua Barat Manokwari & Nabire

Skema RGB	Waktu Penelitian Tgl 12 Nopember 2023	
	Waktu (WIT)	Posisi Wilayah
1. RGB *Day Convective Storms* *Deep precitipating cloud with small & large ice Cb Cloud*	09.00 - 03.00	Biak
2. RGB 24-*hour Microphysics* Awan tebal dengan puncak yang tinggi (Cumulunimbus)	09.00 - 03.00	Papua Barat Manokwari, Biak & Serui
3. RGB *Air Mass* Kandungan massa udara hangat Kandungan uap air yang tinggi	09.00 - 03.00	Papua Barat Manokwari & Biak

Figure 8. Summary of the position of the convective cloud area for the period November 10 - 12, 2023.

Temperature contours of convective cloud tops
June 2023 period

Based on the contour graph of the peak temperature of convective clouds in the coastal area of Cenderawasih Bay for the period June 10-12, 2023, it is found that the dominant peak temperature of the cloud is

at a temperature level of -60 ^{0}C to -70 ^{0}C. This indicates that the peak temperature is the temperature of the cumulus cloud type or cumulunimbus cloud. The dominant convective cloud growth phase time period occurs in the afternoon at 06.00 to 09.00 UTC (15.00 to 18.00 WIT) while the dominant convective cloud maturity phase time period occurs at night to early morning at 12.00 to 18.00 UTC (21.00 to 03.00 WIT) and the dominant convective cloud decay phase time period occurs in the early morning to morning at 19.00 to 21.00 UTC (04.00 to 06.00 WIT).

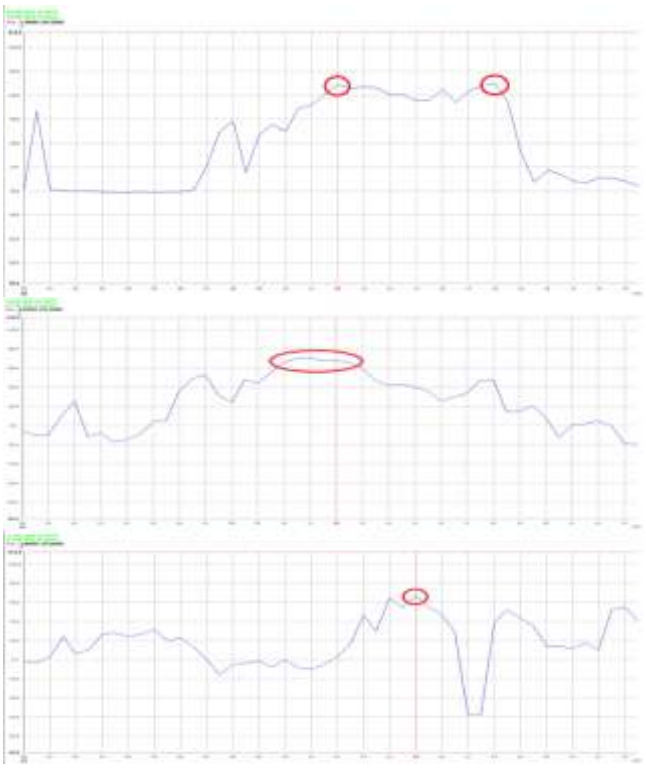

Figure 9. Temperature Contour Graph of Peak Convective Clouds for the Period of June 10-12, 2023

November 2023 period

Based on the contour graph of the peak temperature of convective clouds in the coastal area of Cenderawasih Bay for the period November 10-18, 2023, it is found that the dominant peak temperature of the cloud is at a temperature level of -60 ^{0}C to -70 ^{0}C. This indicates that the peak temperature is the temperature of the cumulus cloud type or cumulunimbus cloud. The dominant convective cloud growth phase time period occurs at night at 13.00 to 15.00 UTC (22.00 to 00.00 WIT) while the dominant convective cloud maturity phase time period occurs in the early morning to morning at 15.00 to 21.00 UTC (00.00 to 06.00 WIT) and the dominant convective cloud decay phase time period occurs in the morning at 22.00 to 23.00 UTC (07.00 to 08.00 WIT).

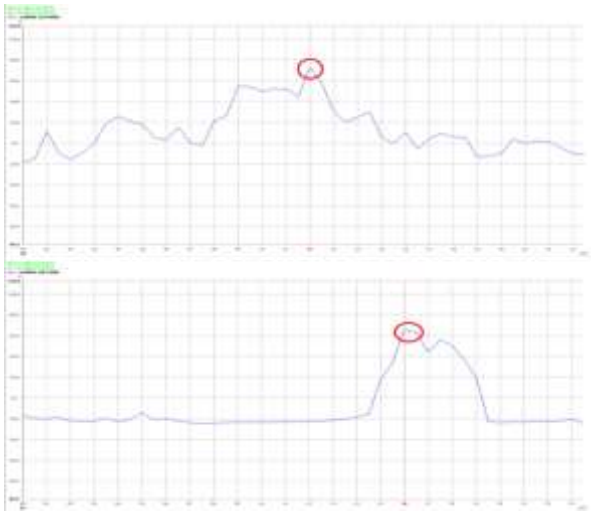

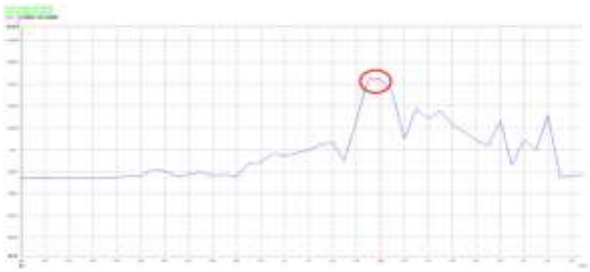

Figure 10. Temperature Contour Graph of Peak Convective Clouds for the Period of November 10-12, 2023

Direction of movement of convective clouds

June 2023 period

Based on the image of the direction of movement of convective clouds in the coastal area of Cenderawasih Bay for the period June 10-12, 2023, it is found that the direction of movement of the dominant convective clouds moves from the east to the west.

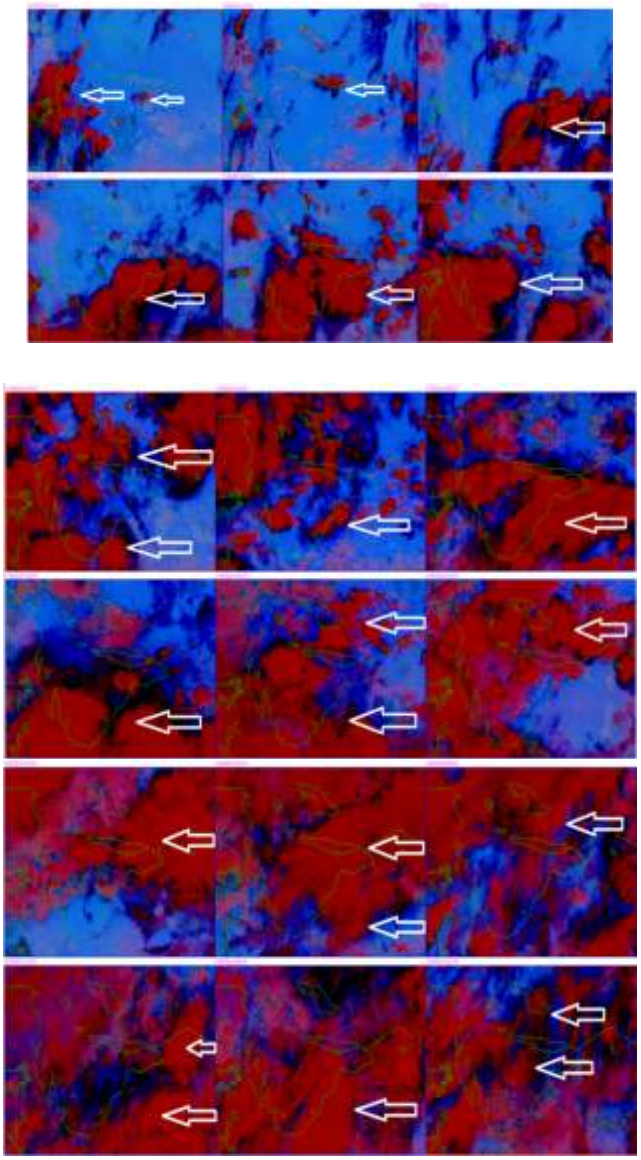

Figure 11. The direction of movement of convective clouds for the period of June 10-12, 2023

November 2023 period

Based on the image of the direction of movement of convective clouds in the coastal region of Cenderawasih Bay for the period November 10-12, 2023, it is found that the direction of movement of convective clouds predominantly moves from the east towards the west, only a few specific time periods of convective cloud movements, moving from west to east.

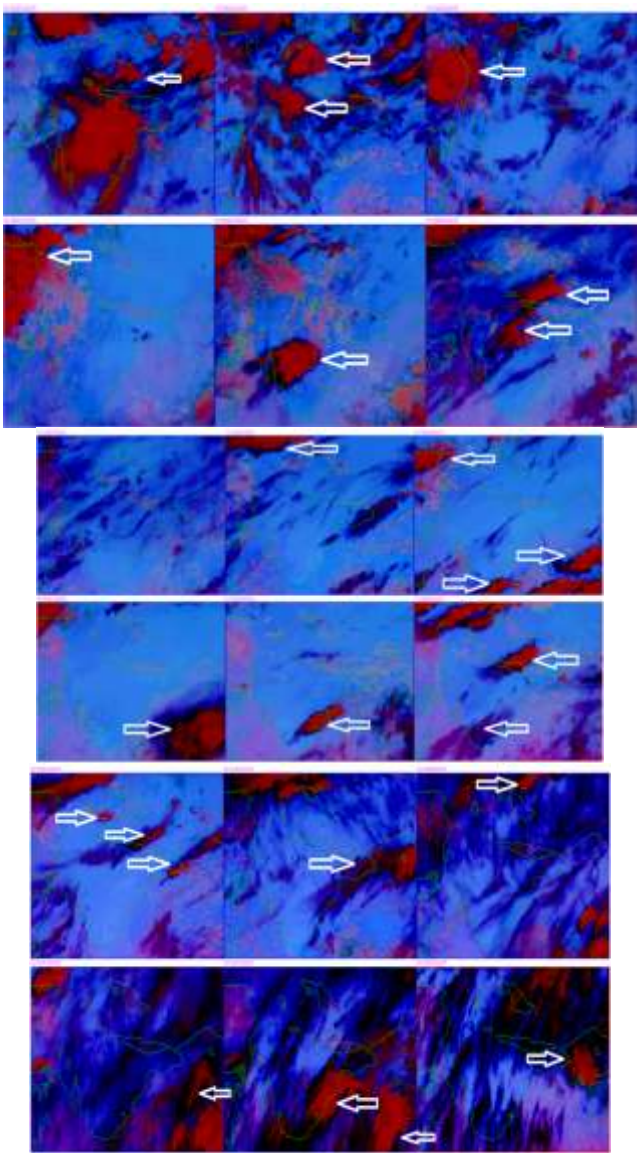

Figure 12. The direction of movement of convective clouds for the period of November 10-12, 2023

Growth phase, mature phase and decay phase of convective clouds

Convective cloud height

Based on the conversion table of cloud top height from cloud top temperature values (Kurniawan et al., 2012):

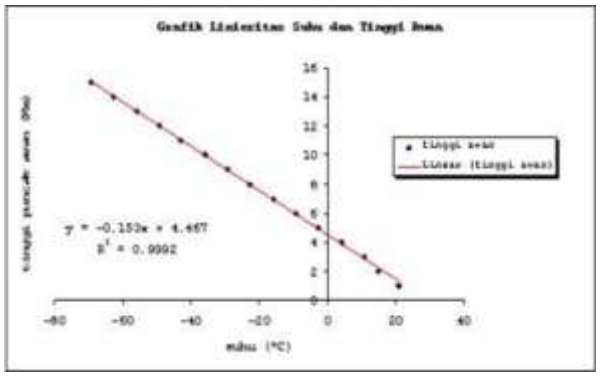

Figure 13. Graph of temperature linearity and cloud height

Based on the data in the image above, using the linear equation **y = -0.152x + 4.467,** where y = cloud height and x = cloud top temperature.

June 2023 period

Based on the cloud peak temperature brightness data for the period June 10-12, 2023 above, it is found

that the dominant convective cloud growth phase occurs with cloud peak temperatures reaching a range of 9.0 to -14.8 ^{0}C, this indicates a cloud height of about 3,100 to 6.700 m (3.1 to 6.7 km). In the mature phase the dominant convective clouds occur with cloud top temperatures reaching a range of -66.8 to -70.4 ^{0}C, this indicates a cloud height of about 14.700 to 15,200 m (14.7 to 15.2 km) while the decay phase of the dominant convective clouds occurs with cloud top temperatures reaching 5.3 to -12.5 ^{0}C. This indicates a cloud height of about 3.700 to 6.400 (3.7 to 6.4 km).

Figure 14. Brightness of cloud peak temperature (a) growing phase, (b) mature phase and (c) decay phase for the period June 10-12, 2023

November 2023 period

Based on the cloud peak temperature brightness data for the period November 10-12, 2023 above, it is found that the dominant convective cloud growth phase occurs with cloud peak temperatures reaching the range of 2.5 to -13.8 ^{0}C, this indicates a cloud height of about 4.100 to 6.600 m (4.1 to 6.6 km). In the mature phase the dominant convective clouds occur with cloud top temperatures reaching a range of -51.0 to -66.4 ^{0}C, this indicates a cloud height of about 12.300 to 14.600 m (12.3 to 14.6 km) while the phase of convective cloud decay is dominant with cloud top temperatures reaching 17.3 to -13.3 ^{0}C. This indicates a cloud height of about 1.800 to 6.500 (1.8 to 6.5 km).

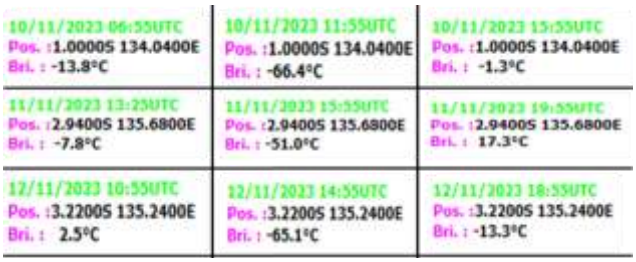

Figure 15. Brightness of cloud peak temperature (a) growing phase, (b) mature phase and (c) decay phase for the period November 10-12, 2023

Histogram of cloud peak temperature percentage
June 2023 period

Based on the histogram graph of the percentage of cloud peak temperature for the period June 10-12, 2023, it is found that in the growing phase (a) the histogram of the percentage of dominant cloud peak temperatures ranges from 14.5 % - 41.9 %, the mature phase (b) the histogram of the percentage of dominant cloud peak temperatures ranges from 41.6 % - 49.3 % and the decay phase (c) the histogram of the percentage of dominant cloud peak temperatures ranges from 19.4 % - 30.9%.

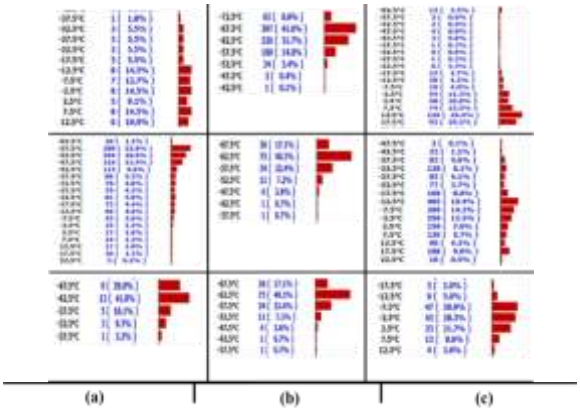

Figure 16. Histogram of cloud peak temperature percentage (a) growing phase, (b) mature phase and (c) decay phase for the period June 10-12, 2023

November 2023 period

Based on the histogram graph of the percentage of cloud peak temperature for the period November 10-

12, 2023, it is found that in the growing phase (a) the histogram of the percentage of dominant cloud peak temperature ranges from 20.7 % - 42.3 %, the mature phase (b) the histogram of the percentage of dominant cloud peak temperature ranges from 24.8 % - 43.2 % and the decay phase (c) the histogram of the percentage of dominant cloud peak temperature ranges from 14.0 % - 25.9 %.

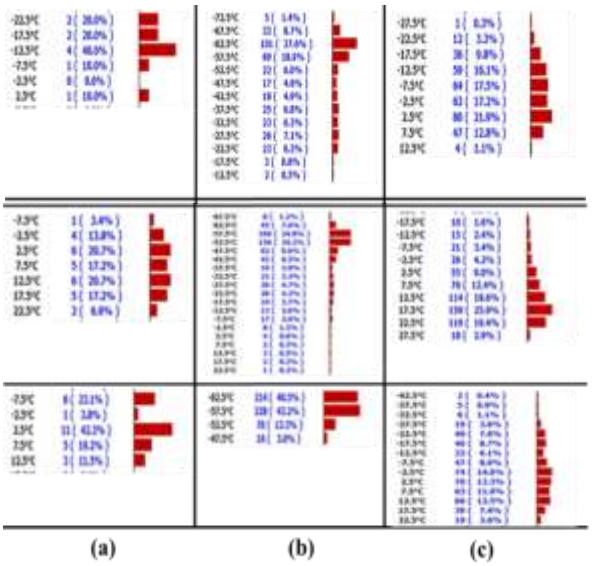

Figure 17. Histogram of cloud peak temperature percentage (a) growing phase, (b) mature phase and (c) decay phase for the period Nopember 10-12, 2023

Convective cloud distance coverage

June 2023 period

Based on the brightness of the convective cloud distance coverage for the period June 10-12, 2023, it was found that in the growing phase (a) the dominant convective cloud distance coverage ranged from 16 - 92 km, the mature phase (b) the dominant convective cloud distance coverage ranged from 50 - 132 km and the decay phase (c) the dominant convective cloud distance coverage ranged from 22 - 49 km.

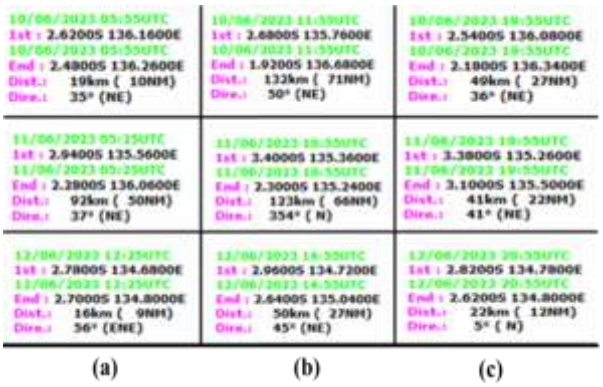

Figure 18. Convective cloud distance coverage (a) growing phase, (b) mature phase and (c) decay phase for the period June 10-12, 2023

Nopember 2023 period

Based on the brightness of the convective cloud distance coverage for the period November 10 - 12, 2023, it was found that in the growing phase (a) the dominant convective cloud distance coverage ranged from 9 - 27 km, the mature phase (b) the dominant convective cloud distance coverage ranged from 35 - 135 km and the decay phase (c) the dominant convective cloud distance coverage ranged from 17 - 71 km.

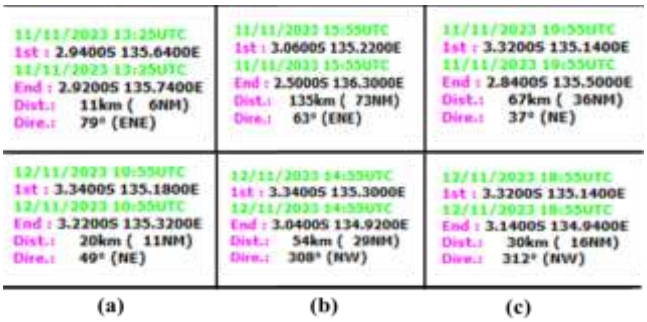

Figure 19. Convective cloud distance coverage (a) growing phase, (b) mature phase and (c) decay phase for the period Nopember 10-12, 2023

The relationship between convective cloud distribution variables and rainfall variables
Comparison of composite color area
Sample period June 10, 2023

Based on the RGB composite color area comparison image, the sample period of June 10, 2023, it is found that the largest RGB area result is the RGB day convective storms area, while the smallest RGB area is the RGB false composite color area. This indicates that with the largest area of RGB day convective storms, it is ideal for identifying convective clouds and strong rising air currents during the day, detecting ice particles at the top of the cloud, so that it has a strong relationship with rainfall variables that will fall in a certain area.

Figure 20. Com—

Sample period Nopember 10, 2023

Based on the RGB composite color area comparison image, the sample period November 10, 2023, it is found that the largest RGB area result is the RGB 24-hour Microphysics area, while the smallest RGB area is the RGB false composite color area. This indicates that with the largest area result from RGB 24-hour Microphysics, the accuracy in monitoring the convective cloud development cycle that applies day and night (24 hours), monitoring the difference in cloud top temperature which is useful in identifying potential bad weather, which can be related to rainfall variables in a particular area.

Figure 21. Comparison of area results of (a) daily convective storm RGB, (b) 24-hour microphysical RGB and (c) air mass RGB, sample period Nopember 10, 2023

Spatial Distribution
Spatial map of rainfall
June 2023 period

Based on the spatial map of rainfall (mm) for the period June 10-12, 2023, it is found that the highest rainfall is found in the southern coastal area of Cenderawasih Bay, namely the Nabire area, while the lowest rainfall is found in the northern coastal area of Cenderawasih Bay, namely the Manokwari and Serui areas. This indicates that in the period of June 10-12, 2023, the highest rainfall is dominant in the southern part of Cenderawasih Bay.

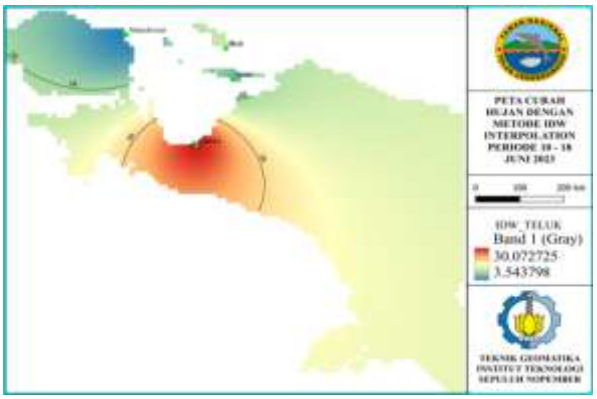

Figure 22. Spatial map of rainfall for the period of June 10-12, 2023

Nopember 2023 period

Based on the spatial map of rainfall (mm) for the period November 10-12, 2023, it is found that the highest rainfall is found in the northern coastal area of Cenderawasih Bay, namely the Manokwari and Serui areas, while the lowest rainfall is found in the southern coastal area of Cenderawasih Bay, namely the Nabire area. This indicates that in the period November 10-12, 2023, the highest rainfall is dominant in the northern part of Cenderawasih Bay.

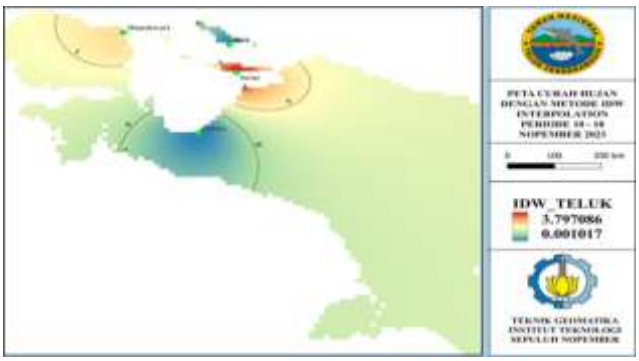

Figure 23. Spatial map of rainfall for the period of November 10-12, 2023
Spatial map of convective cloud distribution

June 2023 period

Based on the spatial map image of convective cloud distribution for the period June 10-12, 2023, it is obtained that the most dominant convective cloud distribution occurs in the northern and southern coastal areas of Cenderawasih Bay, namely the Manokwari and Nabire areas while the lack of convective cloud distribution occurs in the central coastal area of Cenderawasih Bay, namely the Serui area.

Nopember 2023 period

Based on the spatial map of convective cloud distribution for the period November 10-12, 2023, it is found that the most dominant convective cloud distribution occurs in the northern coastal area of Cenderawasih Bay, namely the Manokwari area while the lack of convective cloud distribution occurs in the central and southern coastal areas of Cenderawasih Bay, namely the Serui and Nabire areas.

Spatial map of the dominant position of convective cloud growth

Based on the spatial map image of the dominant position of convective cloud growth for the period June 10-12, 2023 and November 10-12, 2023, it is found that the dominant position of convective cloud growth occurs in the mid and southern coastal areas of Cenderawasih Bay, namely the Nabire area.

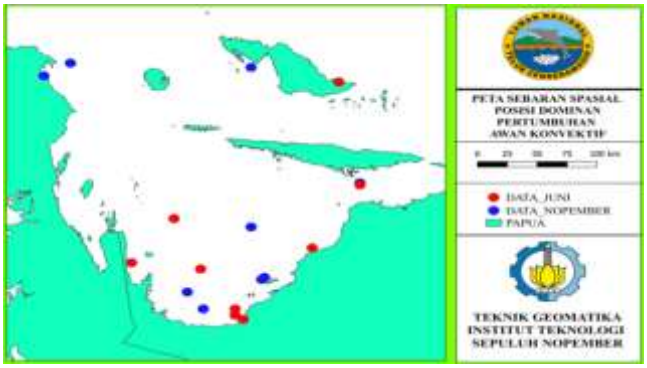

Figure 24. Spatial map of the dominant position of convective cloud growth

3D Overlay Map (Three Dimensions)
June 2023 period

Based on the 3D (Three-Dimensional) overlay map image of convective clouds for the period June 10-12, 2023, there is a dominant high and thick vertical convective cloud structure in almost all coastal areas of Cenderawasih Bay. Identification of active convective clouds can help recognize convective cloud systems that have the potential for severe weather including: heavy rain, thunderstorms and others.

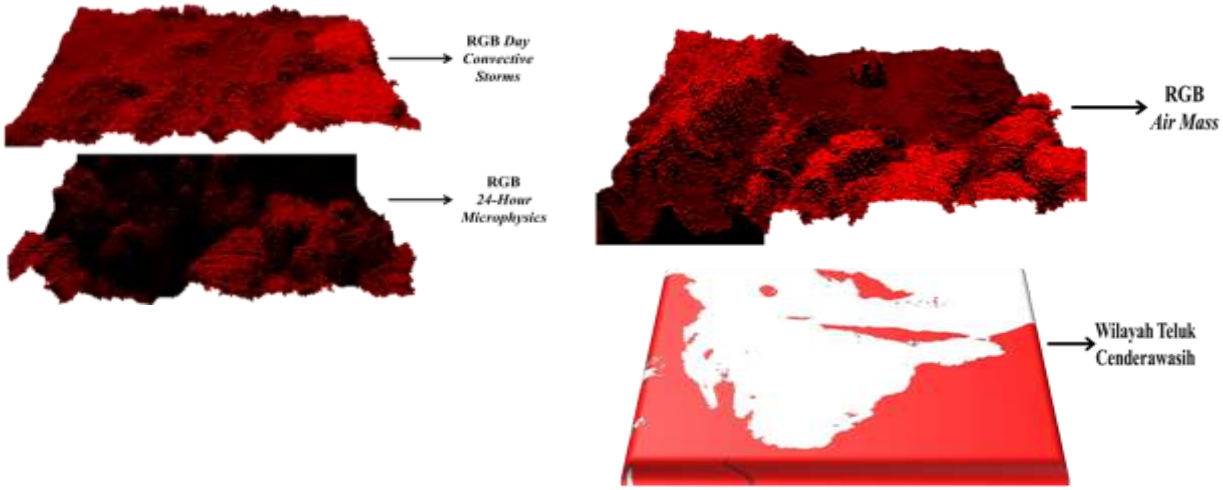

Figure 25. 3D Overlay Map for the period June 10-12, 2023

Nopember 2023 period

Based on the image of the 3D overlay map (Three Dimensions) of convective clouds for the period November 10-12, 2023, it appears that there is a lack of dominant high and thick vertical convective cloud structures in the coastal area of Cenderawasih Bay. Identification of active convective clouds can help recognize

convective cloud systems that have the potential for severe weather including: heavy rain, thunderstorms and others.

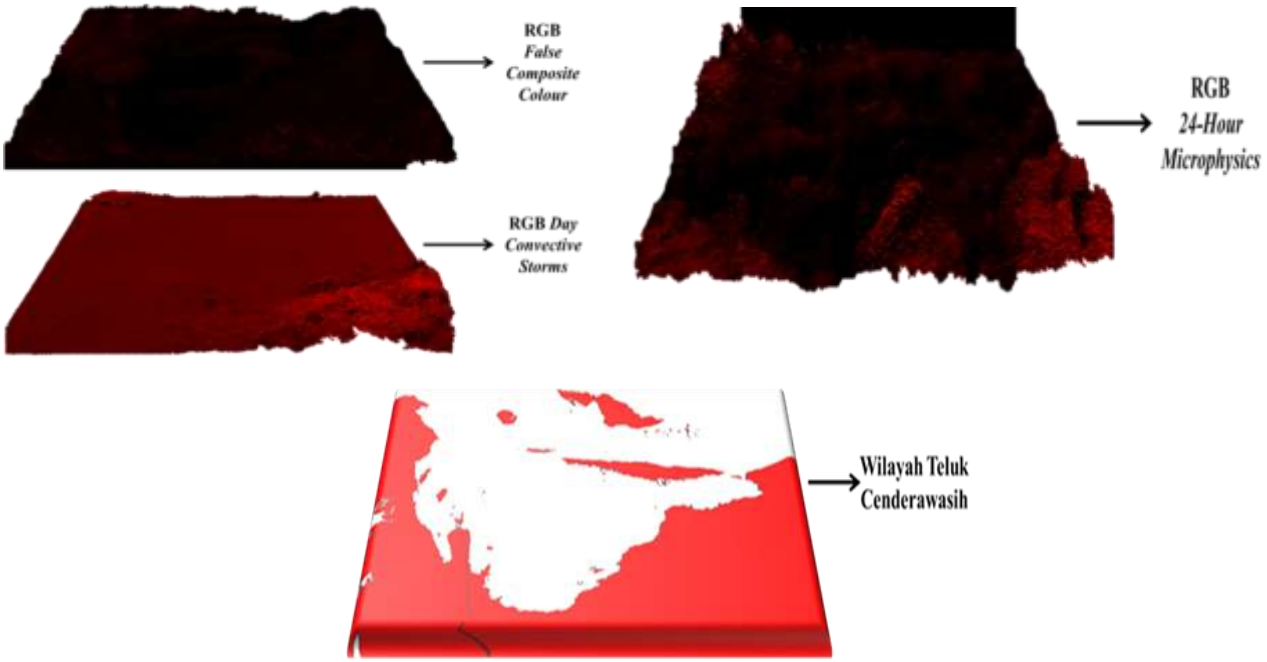

Figure 26. 3D Overlay Map for the period Nopember 10-12, 2023

Crossed wavelet transform (XWT) and wavelet transform coherence (WTC)
June 2023 period
Nabire Region

In the low zone, the dominant interpretation of yellow and green colors, has a strong relationship between the two signals at high frequencies. The direction of the phase vector arrow indicates that there is a phase difference, one variable signal tends to precede the other variable. In the middle zone, dominant light color interpretation, there is some correlation but weaker than high frequency. The direction of the phase vector arrow shows the direction of the vector is more varied, reflecting a relationship that is not always consistent. In the high zone, dominated by the dark blue color interpretation, there are not many significant relationships between the variable signals at large time scales (low frequency). The phase vector direction remains visible but does not lead to a strong pattern indicating a weak relationship. There is a strong and significant correlation between the convective cloud distribution variable and the rainfall variable, at low periods (high frequency). The correlation becomes weaker at long periods (low frequency). The causal relationship between convective cloud variables and rainfall is shown by the direction of the dominant phase vector arrow towards the bottom left (quadrant III). This means that rainfall leads clouds where rainfall variables precede, cloud variables decline in the middle zone (anti-phase relationship). In the low zone, the phase vector arrow direction is dominant in the lower right arrow direction (quadrant II). This means that rainfall leads clouds where rainfall variables and cloud variables rise together but rain occurs first (in-phase relationship). In the high zone, the dominant phase vector arrow direction is the upper right arrow (quadrant I). This means that the cloud amount variable causes rain directly in the high zone. The in-phase relationship is strong, meaning that the increase in clouds is in line with the increase in rain.

Biak region

The most significant relationship between the two variables occurs in the period in the middle zone, which is consistent throughout time. There is synchronization of the variables at some parts of time at low frequencies. The direction of the phase vector arrows in the low zone shows that there is a lot of variation in the direction of the arrows, which means that the variables are synchronized with each other. Multiple diagonal or downward arrows: indicates time shifts between signals. The causal relationship between the convective cloud variables and rainfall is shown by the direction of the dominant phase vector arrow towards the bottom right (quadrant II) in the middle zone. This indicates that the relationship is in-phase (positive relationship between cloud & rain), dominant rainfall leads the number of clouds. In the low zone, the direction of the phase vector arrow tends to vary. This indicates an unstable relationship or opposite phase.

Serui Region

There is a strong relationship between the two variables in the mid-zone daily period. The variables have stable synchronization at most times and intermediate frequencies. The dominant direction of the phase vector arrows indicates the signals are often in nearly synchronous phase or the first signal is slightly ahead. In some sections there are upward arrows indicating the second signal is ahead. The causal relationship between convective cloud variables and rainfall is shown by the direction of the dominant phase vector arrow toward the lower right of quadrant II, indicating the relationship between clouds and rain is in-phase, and rainfall tends to lead the number of clouds. In the low zone, the direction of the phase vector arrow is more variable, indicating an unstable relationship or opposite phase.

Manokwari Region

There is a strong relationship between the two variables at short periods (2-6), but it is limited to a certain time span (time index 3-7). The absence of a dominant synchronous pattern at mid-to-high frequencies suggests that the process is more localized, fast and dynamic. The direction of the phase vector arrows indicates that the two variable signals do not seem to move together, but rather precede or overtake each other variably, suggesting more complex dynamics. The causal relationship between convective cloud variables and rainfall is shown by the direction of the dominant phase vector arrow towards the upper left (quadrant III). This means that rainfall leads clouds where rainfall variables precede, cloud variables decrease in the middle zone (anti-phase relationship). In the low zone and high zone, the phase vector arrow direction is dominant in the direction of the lower right arrow (quadrant II). This means that rainfall leads clouds where rainfall variables and cloud variables rise together but rain occurs first (in-phase relationship).

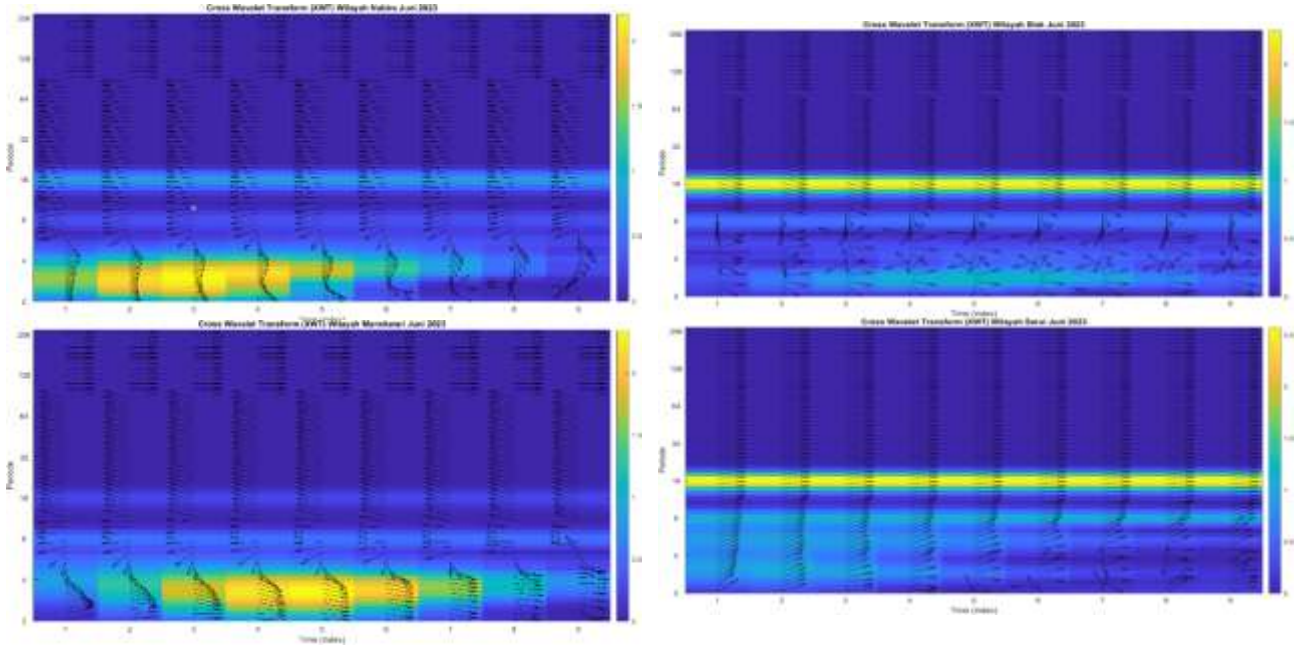

Figure 27. Results of cross wavelet transform (XWT) (a) Nabire region, (b) Biak region, (c) Serui region, and (d) Manokwari region, period June, 2023

Nopember 2023 period

Serui Region

There is a strong relationship seen in the low to medium period (4 - 8 days) between index times 5-9 showing a consistent and strong relationship between the amount of clouds and rainfall in that short period. In the middle zone (16-day period) the interpretation of yellow color, but relatively narrow. The causal relationship between convective cloud variables and rainfall is indicated by the direction of the dominant phase vector arrows in the upper right and lower right directions (quadrants I and II) in the high and medium zones. This means that the variable number of clouds causes rainfall directly. The in-phase relationship is strong, meaning that the increase in clouds is in line with the increase in rain and the rainfall variable leads the clouds where the rainfall variable and the cloud variable rise together but the rain occurs first (in-phase relationship).

Manokwari Region

There is a strong relationship seen in the yellow color interpretation appears in the low zone (period 4 days) between time index 2 - 6, also seen green - yellow color interpretation in the low zone (period 8 days) around time index 2 - 5. In the middle zone (period 16 days) shows a moderate relationship (green color interpretation) indicates not dominant. The causal relationship between convective cloud variables and rainfall is indicated by the direction of the dominant phase vector arrow towards the upper right (quadrant I). This means that the variable number of clouds causes rainfall directly in the high, medium and low zones. The in-phase relationship is strong, meaning that the increase in clouds is in line with the increase in rain.

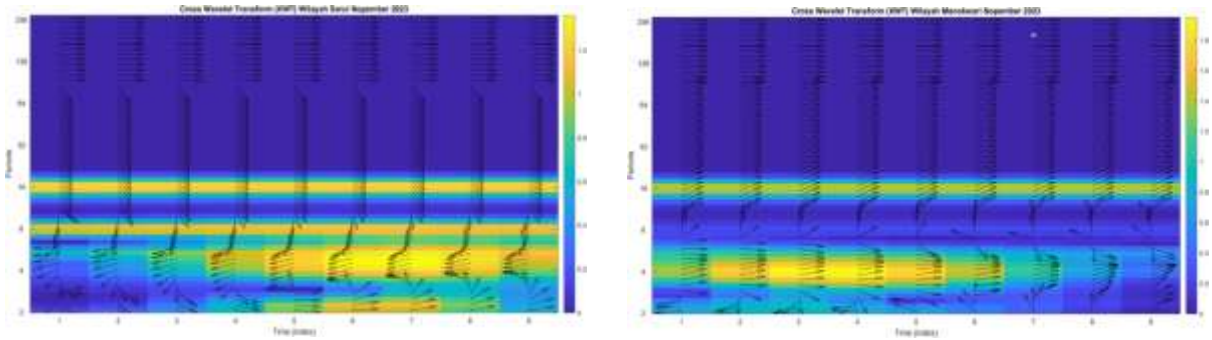

Figure 28. Results of cross wavelet transform (XWT) (a) Serui region, (b) Manokwari region, period June, 2023

Nabire Region

In the middle zone, the dominant intensity of yellow color indicates high coherence, indicating a strong and consistent relationship between convective cloud distribution variables and rainfall variables. In the low zone, the dominant intensity is interpreted as blue or purple, indicating low coherence. The direction of the dominant phase vector arrow is to the right, meaning that the relationship between the two variables moves in the same direction. Some arrows in the low zone point upwards and to the left and are mixed, indicating a lack of synchronization in the relationship between the variables. The causal relationship between the variables of convective clouds and rainfall is indicated by the direction of the dominant phase vector arrow toward the upper right (quadrant I). This means that the variable number of clouds causes rainfall directly in the high, medium and low zones. The in-phase relationship is strong, meaning that the increase in clouds is in line with the increase in rain.

Biak region

In the middle zone there is a very strong and stable relationship between the two variables. This indicates that on a large period scale (low frequency), the two variables show a strong correlation over time. In the low zone, the coherence can drop to below 0.3, meaning that the relationship between the two variables is very weak over short periods, indicating that there is a short-term disturbance in the relationship that could be another influencing variable. The direction of the phase vector arrow pointing to the right indicates the dominant phase relationship of the two variables rising and falling together. In the low zone (short period), it starts to look more random indicating a change in the dynamics of the relationship, a delay, or even an inverse relationship. The causal relationship between the variables of convective clouds and rainfall is indicated by the direction of the dominant phase vector arrow towards the upper right (quadrant I). This means that the variable number of clouds causes rainfall directly in the high, medium and low zones. The in-phase relationship is strong, meaning that an increase in clouds goes hand in hand with an increase in rain.

Serui Region

In the middle zone, high coherence is stable for most of the time period. This means that the medium - high term relationship is very consistent. The low zone, however, indicates that the coherence may fall below 0.3. Most of the phase vector arrows point to the right, indicating that the two variables are moving together. In the low zone period, it starts to appear that the arrows move randomly indicating an unstable phase. The causal relationship between the variables of convective clouds and rainfall is indicated by the direction of the phase vector arrows predominantly towards the upper right (quadrant I). This means that the variable number of clouds causes rainfall directly in the high, medium and low zones. The in-phase relationship is strong, meaning that the increase in clouds is in line with the increase in rain.

Manokwari Region

In the middle to upper zone shows almost perfect coherence (0.95-1), indicated by the overall yellow color interpretation. This means that there is a very strong and stable relationship between the two variables in the medium to long term. In the lower zone, the bluer color interpretation indicates moderate to low coherence (0.5-0.7). This indicates that the relationship between the variables becomes more unstable in the short term. The

direction of the phase vector arrow to the right in almost all periods and times, indicates that the two variables move together (synchronously) while in the lower low zone, the direction of the phase vector arrow moves randomly. The causal relationship between the convective cloud variables and rainfall is indicated by the direction of the dominant phase vector arrow to the upper right (quadrant I). This means that the variable amount of clouds causes rain directly in the high, middle and low zones. The in-phase relationship is strong, meaning that the increase in clouds is in line with the increase in rain.

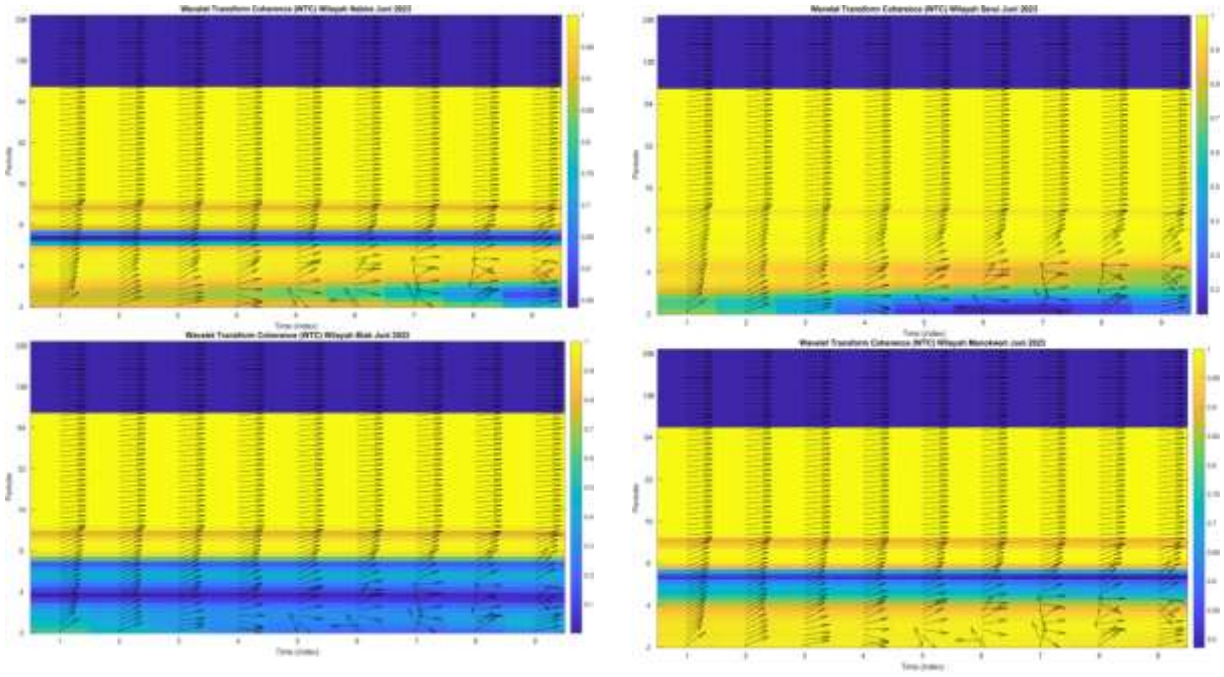

Figure 29. Results of wavelet transform coherence (WTC) (a) Nabire region, (b) Biak region, (c) Serui region, and (d) Manokwari region, period June 2023

Nopember 2023 period

Serui Region

In the low to medium zone, the interpretation of the bright yellow color shows a strong coherence between the two variables, indicating that both variables have significant occurrences in the time scale. In the high zone, the dominant dark blue color intensity indicates no significant coherence in the long term. The causal relationship between the convective cloud variables and rainfall is shown by the direction of the dominant phase vector arrows in the upper right and lower right directions (quadrants I and II) in the high and medium zones. This means that the cloud amount variable causes rain directly.

The in-phase relationship is strong, meaning that the increase in clouds is in line with the increase in rain and the rainfall variable leads the clouds where the rainfall variable and the cloud variable increase together but rain occurs first (in-phase relationship). In the low zone, the direction of the dominant phase vector arrow is in the lower left direction (quadrant III). This means that rainfall leads the clouds where the rainfall variable precedes, the cloud variable decreases in the medium zone (anti-phase relationship).

Manokwari Region

In the low to medium zone, the interpretation of the bright yellow color indicates a strong coherence between the two variables. In the high zone, the dominant dark blue color intensity indicates no significant coherence in the long term. The causal relationship between the convective cloud variables and rainfall is indicated by the direction of the dominant phase vector arrows in the upper right and lower right directions (quadrants I and II) in the high and medium zones. This means that the cloud amount variable causes rain directly. The in-phase relationship is strong, meaning that the increase in clouds is in line with the increase in rain and the rainfall variable leads the clouds where the rainfall variable and the cloud variable increase together but rain occurs first (in-phase relationship). In the low zone, the direction of the dominant phase vector arrow is in the lower left direction (quadrant III). This means that rainfall leads the clouds where the rainfall variable precedes, the cloud variable decreases in the medium zone (anti-phase relationship).

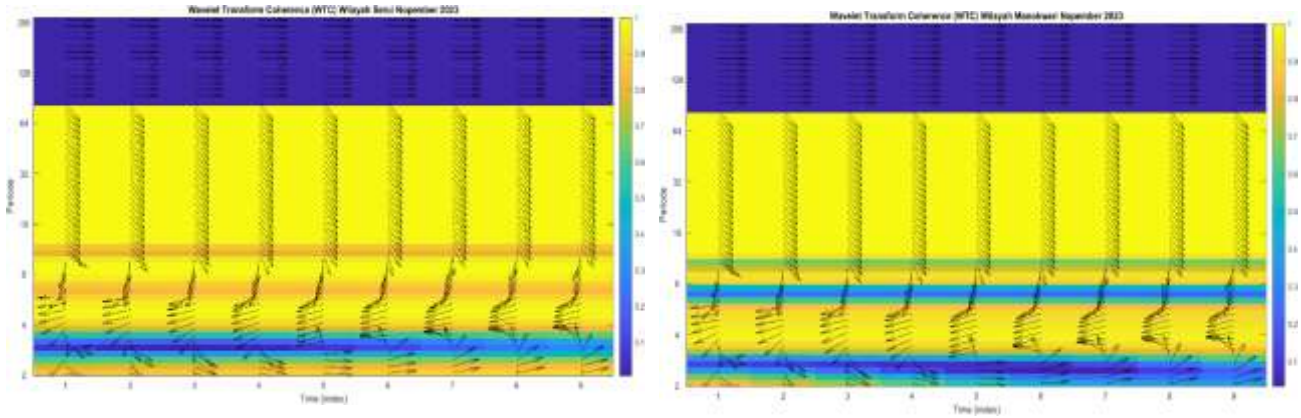

Figure 30. Results wavelet transform coherence (WTC) (a) Serui region, (b) Manokwari region, period Nopember 2023

CONCLUSION

This study concludes that the distribution pattern of convective clouds in the coastal areas of Cenderawasih Bay particularly in Manokwari, Biak, Serui, and Nabire varies significantly between June and November 2023. In June, convective clouds were more dominant and widespread, with peak temperatures ranging from -50°C to -70°C, cloud tops reaching up to 15.2 km, and significant cloud coverage across the coastal zones. Conversely, November showed a decline in convective activity, with reduced cloud height and coverage. The time series analysis reveals that convective cloud development in both periods predominantly occurs during nighttime to early morning, moving east to west. The RGB day convective storm composite proved effective in June for identifying ice particles linked to rainfall, while the RGB 24-hour microphysics product in November highlighted cloud-top temperature differences useful for detecting severe weather potential. 3D image overlays further confirmed the dominance of high, thick convective cloud structures in June compared to November. Additionally, wavelet coherence analysis revealed strong temporal and spatial correlations between convective cloud presence and rainfall intensity, especially in low and mid-frequency zones, with varying in-phase and anti-phase relationships. These findings underscore the importance of satellite-based RGB analysis in enhancing local rainfall prediction and disaster preparedness in Papua's coastal regions. For future research, it is recommended to integrate ground-based radar data and high-resolution numerical weather models to validate satellite observations and improve the accuracy of convective cloud forecasting in other high-rainfall tropical zones.

REFERENCES

Christensen, H. M., & Driver, O. G. A. (2021). The fractal nature of clouds in global storm-resolving models. *arXiv preprint arXiv:2108.08565*. https://arxiv.org/abs/2108.08565

Fujita, M., & Yasunari, T. (2017). Convective cloud distribution over the maritime continent. *Geophysical Research Letters*, *44*(9), 4565–4572.

Huda, A. D., & Mulya, A. (2022). Pemanfaatan Metode Rgb (Red Green Blue) Pada Citra Satelit Himawari-8 Dalam Klasifikasi Awan Pada Kejadian Hujan Lebat Daerah Sidoarjo 3 Februari 2021. *J. Tek. SILITEK*, *1*(02), 73–79. https://doi.org/10.51135/jts.v1i02.14

Ishii, M., & Kachi, M. (2015). Global sea surface temperature analysis using satellite data. *Remote Sensing*, *7*(7), 8658–8672.

Kawamoto, K., & Nakajima, T. (2016). Retrieval of cloud properties using satellite data. *Journal of Geophysical Research: Atmospheres*, *121*(12), 6789–6802.

Kikuchi, K., & Wang, B. (2015). Global perspective of the quasi-biweekly oscillation. *Journal of Climate*, *28*(17), 6637–6654.

Kurniawan, R. D., Abdurrohim, E., Teknik, F., Studi, P., Informatika, T., & Islam, U. (2012). *Perancangan Aplikasi Identifikasi Jenis Awan Dengan Menggunakan Metode Piksel-Fuzzy*. *8*(31), 16–31.

Matsui, T., & Masunaga, H. (2015). Satellite-based estimation of convective cloud top height using Himawari-8 data. *Atmospheric Research*, *160*, 1–10.

Nie, L., Chen, Y., Du, M., Sun, C., & Zhang, D. (2023). A knowledge-based data-driven (KBDD) framework for all-day identification of cloud types using satellite remote sensing. *arXiv preprint arXiv:2312.00308*. https://arxiv.org/abs/2312.00308

Ninggar, R. R., Siregar, D. C., & Perdana, I. F. P. (2023). Analisis Pola Distribusi Awan Konvektif di Wilayah Provinsi Banten Berbasis Radar Cuaca Convective Cloud Distribution Patterns in Banten Using Weather Radar Data. *Bul. Meteorol. Klimatologi, dan Geofis.*, *4*(6), 35–43.

Nugroho, G. A. (2017). RGB Himawari Satellite Data before Localized Heavy Rain March 17 2017 Bandung Basin

Indonesia. *Google Scholar Citations*. https://scholar.google.com/citations?hl=en&user=uVgsBn0AAAAJ

Ohashi, Y., & Kida, H. (2018). Analysis of convective cloud patterns using satellite data. *Journal of Climate*, *31*(4), 1234–1245.

Paski, J. A. I., Sepriando, A., & Pertiwi, D. A. S. (2019). Pemanfaatan Teknik Rgb Pada Citra Satelit Himawari-8 Untuk Analisis Dinamika Atmosfer Kejadian Banjir Lampung 20 - 21 Februari 2017. *J. Meteorol. Klimatologi dan Geofis.*, *4*(3), 8–15. https://doi.org/10.36754/jmkg.v4i3.48

Ramdani, R. F. (2021). Analisis Kejadian Hujan Lebat dan Banjir Kabupaten Pati Menggunakan Metode Cloud Convective Overlays dan Red Green Blue Convective Storms pada Satelit Himawari 8. *J. Penelit. Sains*, *23*(3), 150. https://doi.org/10.56064/jps.v23i3.647

Romero Jure, P. V, Masuelli, S., & Cabral, J. B. (2023). A labeled dataset of cloud types using data from GOES-16 and CloudSat. *arXiv preprint arXiv:2306.11159*. https://arxiv.org/abs/2306.11159

Rouw, A., Hadi, T. W., K, B. T. H., & Hadi, S. (2014). Analisis Variasi Geografis Pola Hujan di Wilayah Papua Geographic Variation Analysis of Rainfall Pattern in Papua Region. *J. Tanah dan Iklim*, *38*(1), 25–34.

Saragih, I. J. A., & al., et. (2021). Utilization of Red-Green-Blue (RGB) modification composite for nighttime convective cloud monitoring over North Sumatra region. *IOP Conf. Ser. Earth Environ. Sci.*, *893*(1), 0–11. https://doi.org/10.1088/1755-1315/893/1/012019

Sugiura, N., & Nakajima, T. (2015). Retrieval of cloud microphysical properties from satellite data using a neural network. *Journal of Applied Meteorology and Climatology*, *54*(2), 317–334.

Taniguchi, H., & Nakazawa, T. (2016). Analysis of convective cloud distribution using satellite data. *Journal of the Meteorological Society of Japan*, *94*(3), 123–135.

Xiao, H., Zhang, F., Wang, L., Li, W., Guo, B., & Li, J. (2024). CloudDiff: Super-resolution ensemble retrieval of cloud properties for all day using the generative diffusion model. *arXiv preprint arXiv:2405.04483*. https://arxiv.org/abs/2405.04483

Yamada, M., & Sato, K. (2017). Analysis of cloud distribution patterns using satellite data. *Remote Sensing Letters*, *8*(5), 421–430.

Yoshida, R., & Asano, S. (2015). Retrieval of cloud microphysical properties from satellite data using a neural network. *Journal of Applied Meteorology and Climatology*, *54*(2), 317–334.